Protein Science (1995), *4*:841–848. Cambridge University Press. Printed in the USA.

Structural diversity in a conserved cholera toxin epitope involved in ganglioside binding

MENACHEM SHOHAM,[1] TALI SCHERF,[2] JACOB ANGLISTER,[2]
MICHAEL LEVITT,[3] ETHAN A. MERRITT,[4] AND WIM G.J. HOL[5]

[1] Case Western Reserve University, School of Medicine, Department of Biochemistry, Cleveland, Ohio 44106-4935
[2] The Weizmann Institute of Science, Department of Structural Biology, 76100 Rehovot, Israel
[3] Stanford University, Department of Structural Biology, Stanford, California 94305
[4] Department of Biological Structure, University of Washington, Seattle, Washington 98195
[5] Departments of Biological Structure and Biochemistry, SM-20, and Howard Hughes Medical Institute, University of Washington, Seattle, Washington 98195

(RECEIVED December 22, 1994; ACCEPTED February 21, 1995)

Abstract

Cholera is a widespread disease for which there is no efficient vaccine. A better understanding of the conformational rearrangements at the epitope might be very helpful for the development of a good vaccine. Cholera toxin (CT) as well as the closely related heat-labile toxin from *Escherichia coli* (LT) are composed of two subunits, A and B, which form an oligomeric assembly AB_5. Residues 50–64 on the surface of the B subunits comprise a conserved loop (CTP3), which is involved in saccharide binding to the receptor on epithelial cells. This loop exhibits remarkable conformational plasticity induced by environmental constraints. The crystal structure of this loop is compared in the free and receptor-bound toxins as well as in the crystal and solution structures of a complex with TE33, a monoclonal antibody elicited against CTP3. In the toxins this loop forms an irregular structure connecting a β-strand to the central α-helix. Ser 55 and Gln 56 exhibit considerable conformational variability in the five subunits of the unliganded toxins. Saccharide binding induces a change primarily in Ser 55 and Gln 56 to a conformation identical in all five copies. Thus, saccharide binding confers rigidity upon the loop. The conformation of CTP3 in complex with TE33 is quite different. The amino-terminal part of CTP3 forms a β-turn that fits snugly into a deep binding pocket on TE33, in both the crystal and NMR-derived solution structure. Only 8 and 12 residues out of 15 are seen in the NMR and crystal structures, respectively. Despite these conformational differences, TE33 is cross-reactive with intact CT, albeit with a thousandfold decrease in affinity. This suggests a different interaction of TE33 with intact CT.

Keywords: antipeptide antibody; conformational rearrangements at the epitope; cholera toxin; flexible loop involved in receptor binding

Cholera toxin (CT) as well as the closely related heat-labile toxin from *Escherichia coli* (LT) are composed of two types of subunits, A and B, which form an oligomeric assembly AB_5 (Sixma et al., 1991). The initial step in the toxin-induced process leading to the symptoms of diarrhea is the attachment of the B subunits to intestinal epithelial cells. Immunogenic moieties on the surface of the B_5 molecule therefore constitute suitable targets for the development of peptide vaccines against cholera. Residues 50–64 of the B subunit form such a surface loop that is entirely conserved between CT and LT (Fig. 1; Kinemage 1). This loop is directly involved in carbohydrate binding to the G_{M1} ganglioside receptor on the surface of epithelial cells (Merritt et al., 1994a). Immunization of laboratory animals with a peptide, CTP3, corresponding to the sequence of residues 50–64, has been shown to cause partial neutralization of CT and LT activities in vitro (Jacob et al., 1983, 1984a, 1984b). A monoclonal antibody, TE33, raised against the same CTP3 peptide, is cross-reactive with cholera toxin in a solid-phase immunosorbent assay (ELISA) (Anglister et al., 1988), but in solution the affinity of the antibody for the toxin is a thousandfold lower than for CTP3 (Scherf et al., 1992).

In this paper we compare the conformation of the epitope in four different structures: the recently determined crystal structures of LT (Sixma et al., 1991, 1992), CT B pentamer (Merritt et al., 1994a), and the TE33–CTP3 complex (Shoham, 1993) as well as the NMR-derived structure of the latter in solution (Scherf et al., 1992).

Reprint requests to: Menachem Shoham, Case Western Reserve University, School of Medicine, Department of Biochemistry, Cleveland, Ohio 44106-4935; e-mail: shoham@biochemistry.cwru.edu.

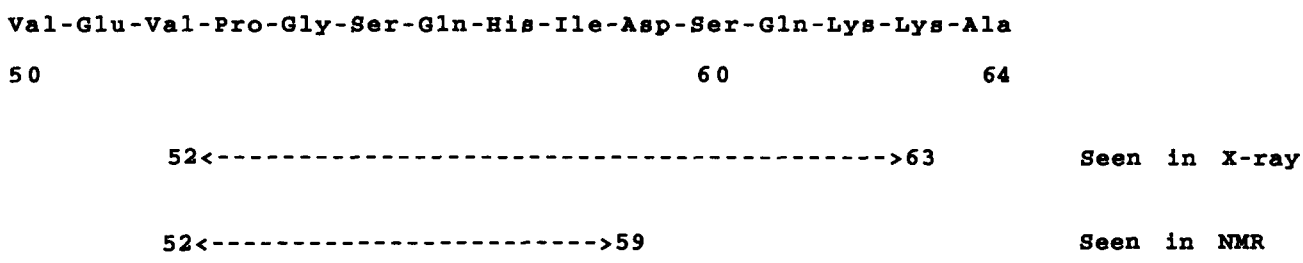

Fig. 1. Sequence of the immunogenic surface peptide CTP3, which is conserved in the B subunits of CT and LT. Overall, the sequence identity between CT and LT is approximately 80%, for both the A and B subunits (Dallas & Falkow, 1980; Yamamoto et al., 1987). Residues of the peptide seen in the X-ray and NMR structures of the peptide–antibody complex are indicated.

The epitope in the crystal structures of LT and CT

The 15 residues of the epitope form a surface loop in both the crystal structures of LT and CT B_5 pentamers. This loop connects a β-strand to the central α-helix of the molecule (Fig. 2; Kinemage 2). The first five residues, Val 50 to Gly 54, are in an extended conformation followed by eight residues that form a loop leading into the α-helix at Lys 62. The side chains of Glu 51 and Gln 61 as well as the carbonyl oxygen atom of Gln 56 form hydrogen bonds to the terminal galactose moiety in receptor-bound toxin structures of CT with the pentasaccharide of the G_{M1} ganglioside as well as in the LT–lactose and LT–galactose complexes (Sixma et al., 1991, 1992). The conformations of the five different copies of these loops in the pentameric toxin–sugar complexes are quite similar to each other, with the largest RMS differences seen for Lys 63 and Ser 55. Moreover, the conformations in galactose–LT, lactose–LT, and G_{M1}–pentasaccharide–CT are very much alike. The unliganded LT structure on the other hand, shows considerably more variability in the coordinates as well as in the thermal parameters of atoms in the epitope. This phenomenon is even more dramatic in the crystal structure of free CT, where there are significant differences in the orientation of certain side chains, in particular of Ser 55 and Gln 56 among the five copies in the B pentamer (E. Westbrook, pers. comm.). In unliganded CT there are in fact three different conformers for Gln 56, one of which corresponds to the unliganded LT conformation (Fig. 3). These conformers differ in the polar interactions of Glu 51, Ser 55, Gln 56, His 57, and Gln 61. The key residue in this network of hydrogen bonds and electrostatic interactions is the imidazole ring of His 57. In free CT it is hydrogen bonded either to a backbone carbonyl oxygen atom of residue 56 or to a combination of the side chains of Glu 51/Ser 55 or to a combination of Glu 51/Gln 56. Interestingly, in unliganded LT there does not seem to be any hydrogen bond donor close enough to the imidazole moiety of His 57, although the amide side-chain atoms of Gln 56 and Gln 61 are within 4 Å of the nitrogen atoms of the imidazole ring. It seems that in unliganded CT this loop can flip between three conformations of nearly equal energy. It is the presence of the bound saccharide moiety that induces a more rigid and more uniform structure onto the epitope loop.

The epitope structure in the TE33–CTP3 immunocomplexes

The structure of the TE33–CTP3 complex has been solved by X-ray crystallography to 2.3 Å resolution (Shoham, 1993) as well as in solution by NMR (Scherf et al., 1992) (Fig. 4; Kinemage 2). Because the size of an Fab fragment (50 kDa) is beyond the range of a two-dimensional NMR structure determination, the conformation of the bound CTP3 was determined by measured NOE distance restraints between CTP3 atoms and selected TE33 moieties and using a calculated model of the latter. This calculated model of the F_v part is quite similar to the X-ray structure with an RMS deviation (RMSD) of 0.85 Å for backbone atoms. The largest differences occur in the complementarity loops L1 and H3, which have RMSDs for backbone atoms of 1.44 and 0.94 Å, respectively. The crystal and NMR structures of bound CTP3 are similar, with an RMSD of 1.63 Å for all common backbone atoms (Table 1; Fig. 5). The first two residues, Val 50 and Glu 51, do not have a fixed conformation either in solution or in the crystalline state. Residues Val 52, Pro 53, Gly 54, and Ser 55 form a β-turn in both structures. The imidazole ring of His 57 is located in an aromatic binding pocket in both structures, made up of Tyr H32 and Trp H100a. The NMR model of bound CTP3 consists of a loop of eight residues, Val 52–Asp 59, with an end-to-end distance of 2.4 Å between Val 52 methyl protons and Asp 59 β-protons. In the crystal structure, Val 52 and Asp 59 are also close to each other with the shortest distance between any two non-hydrogen atoms of these residues being 3.6 Å. The crystal structure of bound CTP3 consists of 12 residues, Val 52–Lys 63. The main discrepancies between the solution and the crystal structure of CTP3 are confined to residues Ser 55 and Gln 56. It is interesting that it is these very same residues that exhibit structural diversity in unliganded CT. In the NMR structure, the side-chain amide group of Gln 56 forms an intramolecular hydrogen bond between its $O\epsilon_1$ atom and the amide nitrogen atoms of Gly 54 and Ser 55, as well as an intermolecular bifurcated hydrogen bond between its $N\epsilon_2$ atom and the guanido NH2 group of Arg H95. In the crystal structure, the side chain of Gln 56 points away from the β-turn into the wall of the antibody-combining site, forming hydrogen bonds and van der Waals contacts with a variety of backbone and side-chain atoms on loops H1 and H2.

What might account for the differences between the crystal and solution structures of bound CTP3? The first issue to consider would be differences in the experimental conditions. The pH of the TE33–CTP3 crystals is 4.0 and the NMR data were collected at pH 7.15. To test the hypothesis that differences in pH might account for the structural differences, the NMR measurements were repeated in the same phosphate buffer as used previously, but at pH 4.0. The NOE distances at pH 4.0 were similar to the values obtained at pH 7.15, with variations of less than 1 Å. The largest changes in distances were, however, con-

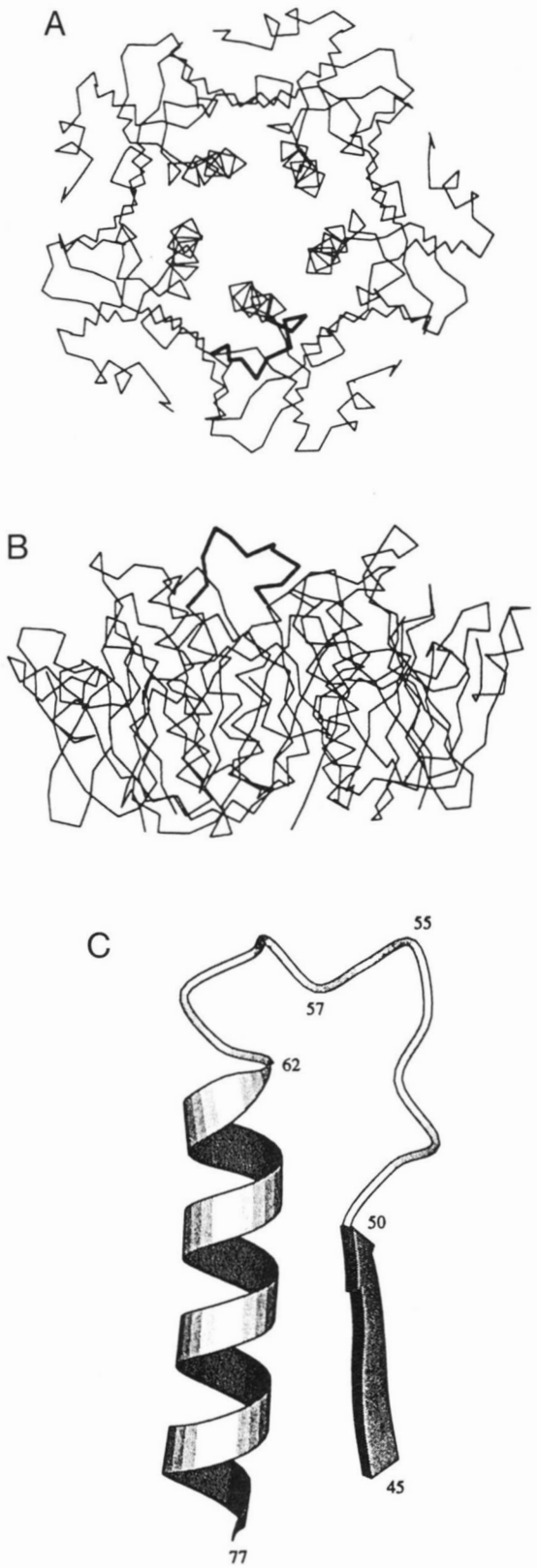

Fig. 2. Immunogenic loop (CTP3) on the surface of the pentameric array of B subunits of the LT from *E. coli*. The CTP3 epitope of one of the subunits is highlighted by thicker lines in these α-carbon diagrams. **A:** View down the fivefold axis. **B:** View perpendicular to the fivefold axis. **C:** Ribbon diagram showing this loop as a link between a β-strand and the central α-helix.

fined to Gln 56 (in its interaction with Trp H50), the very residue that differs the most between the crystal and solution structures. Although in solution the same intermolecular interactions were observed at pH 4.0 and pH 7.15, some conformational changes in the F_v part may occur at the lower pH. Moreover, at least an order of magnitude weaker binding is observed at the lower pH, probably due to protonation of both His 57 of the peptide and His L31 of the antibody.

The second issue to consider is the differences in the complementarity-determining loops of TE33 in crystal and solution. As mentioned earlier, a calculated model of TE33 was used to derive the solution NMR structure of bound CTP3 (Scherf et al., 1992). This calculated model differs from the crystal structure mainly in loops L1 and H3 (Fig. 6). To test whether it is the calculated model that has led to a different solution structure of bound CTP3, the crystal structure of the complex minus the bound peptide was used as a template for docking the peptide under the NMR-derived distance restraints. An initial model of bound CTP3 (residues Val 52–Asp 59) was built manually into the antigen-combining site. Protons were added to the coordinate file, and then the structure was refined by a combination of restrained energy minimization and molecular dynamics calculations as described previously (Scherf et al., 1992). In the refinement only CTP3 residues were allowed to move. This new model for the bound peptide is very similar to the NMR structure derived using the calculated TE33 model with an RMSD of 0.76 and 1.08 Å for main-chain and side-chain atoms, respectively. This NMR model differs from the crystal structure of bound CTP3 mainly in residues Ser 55 and Gln 56, as is the case with the model derived from a calculated TE33 structure. Therefore the use of a calculated model for TE33 cannot be the cause for the difference between the solution and crystal structures of bound CTP3.

The third issue to consider is the presence of a bound citrate ion in the crystal structure of the TE33–CTP3 complex (Fig. 7). This citrate ion is located within van der Waals distance of Pro 53 in between loops L1 and L3. One of the citrate carboxylate groups forms a hydrogen bond with Ser L31a O^{γ}, and

Table 1. *RMSD between respective CTP3 backbone atoms in the four different structures (Å)*[a]

	CTP3–TE33[b] (crystal)	CTP3–TE33[c] (NMR)	CT[d] (crystal)	LT[e] (crystal)
CTP3–TE33 (crystal)	0.0	1.63	3.03	3.06
CTP3–TE33 (NMR)		0.0	2.59	2.59
CT (crystal)			0.0	0.24
LT (crystal)				0.0

[a] Calculations were done with program ALIGN (Satow et al., 1987).
[b] From Shoham (1993); PDB code 1TET.
[c] From Anglister et al. (1988).
[d] For subunit 1 of CT bound to receptor G_{M1} pentasaccharide (Merritt et al., 1994a; PDB code 1CHB).
[e] For subunit 1 of the lactose complex of LT from *E. coli* (Sixma et al., 1992; PDB code 1LTT).

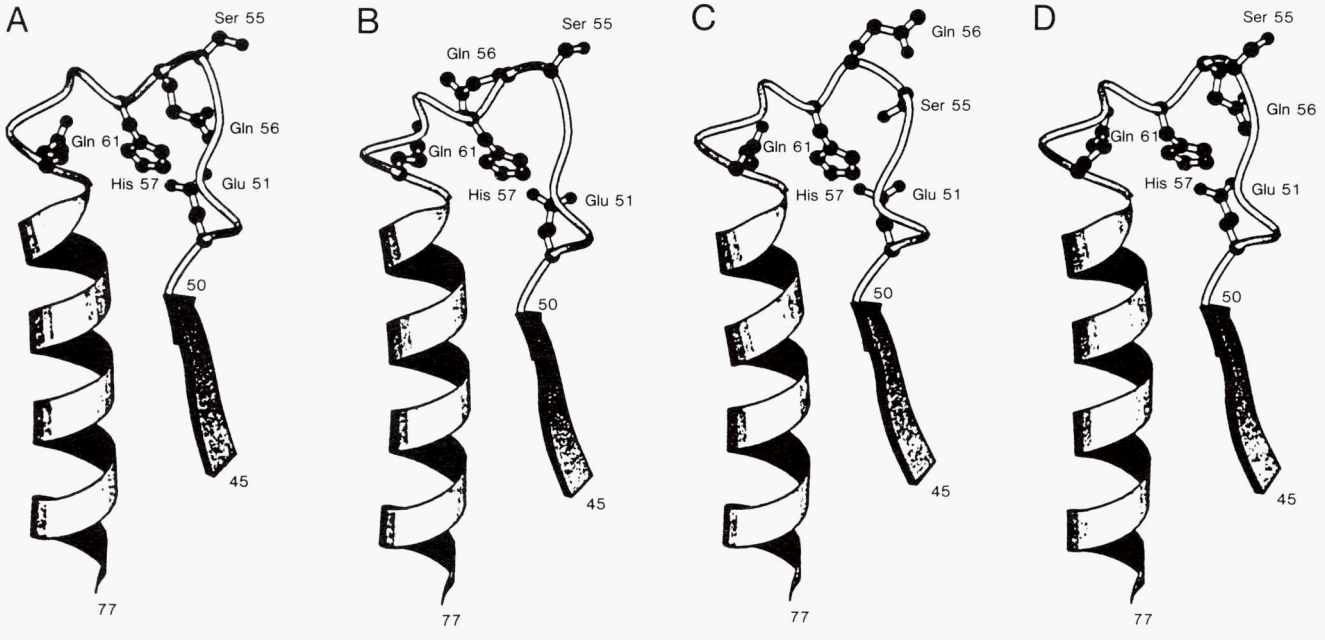

Fig. 3. Ribbon diagram of the CTP3 loop plus preceding strand β_3 (residues 45–50) and subsequent helix α_2 (residues 62–77) in the toxins (**A**) in unliganded LT from *E. coli*. In unliganded CT, there are three different conformers of this loop within the pentameric array of the B subunits (shown in **B**, **C**, and **D**). They differ mostly in the conformation of Ser 55 and Gln 56. Coordinates were kindly provided by Dr. Edwin Westbrook.

two carboxylate groups form salt bridges with the positively charged imidazole rings of His L31 and His L98. In solution His L98 is fully protonated at pH 4, whereas His L31 is only partially protonated (Levy et al., 1989). The interaction with the citrate ion in the crystal may increase the pK of His L31 so that it becomes fully protonated at pH 4. The interaction with citrate may have important consequences for peptide binding because His L31 constitutes part of the surface of the antigen-binding pocket. Loops L1 and H3 do not directly interact with each other in the crystal structure but they do so in the calculated model used for the NMR structure determination (Fig. 6). In the latter model, the rings of Tyr L32 and Trp H100a form a stacking interaction at an interplanar distance of 4 Å. In the crystal structure, on the other hand, Trp H100a is solvent exposed, pointing away from Tyr L32. Trp H100a is the residue that shows the largest discrepancy between the crystal structure and the calculated model, with their respective α-carbon atoms 3.5 Å apart and their respective Cζ_3 atoms 7.6 Å apart. The effect of the bound citrate ion in the crystal structure is to attract polar moieties on loop L1, thereby shortening the distance between Ser L31b O$^{\gamma}$ and Tyr L32 OH to within hydrogen bond

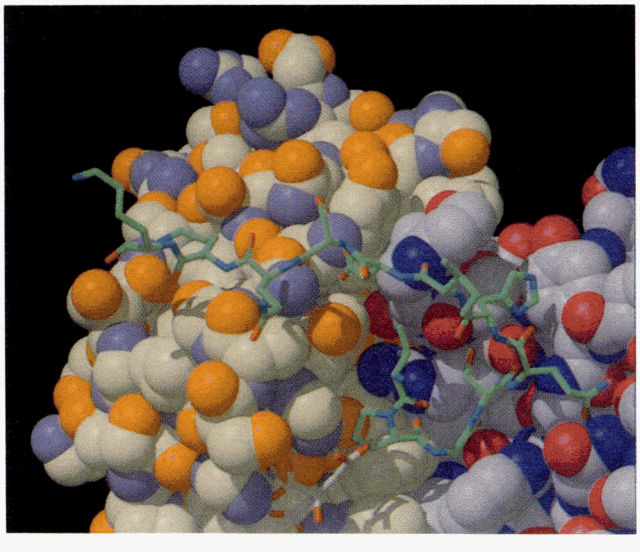

Fig. 4. Residues 50–64 of CT and LT B subunits (CTP3 peptide) bound to the Fab fragment of the anti-CTP3 antibody TE33 in the crystal structure of the complex (Shoham, 1993; PDB code 1TET). The TE33 heavy chain is shown in blue, the light chain in yellow. Only residues 52–63 of the peptide are shown because these are the residues found to be well ordered in the crystal structure. Carbon atoms of the peptide are shown in gray, carbon atoms of a bound citrate ion in white. Figure generated using Raster3D version 2.0 (Merritt & Murphy, 1994).

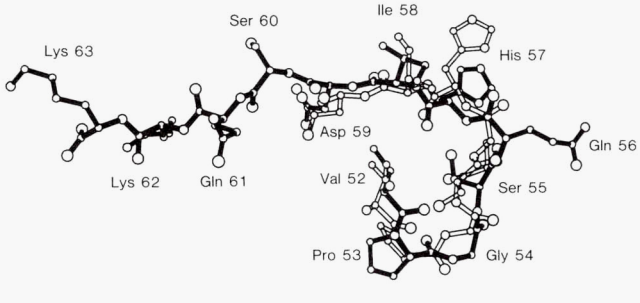

Fig. 5. Superposition of the crystal structure (solid lines) and the NMR structure (open lines) of CTP3 in its complex with the Fab part of a monoclonal antibody, TE33, elicited against CTP3.

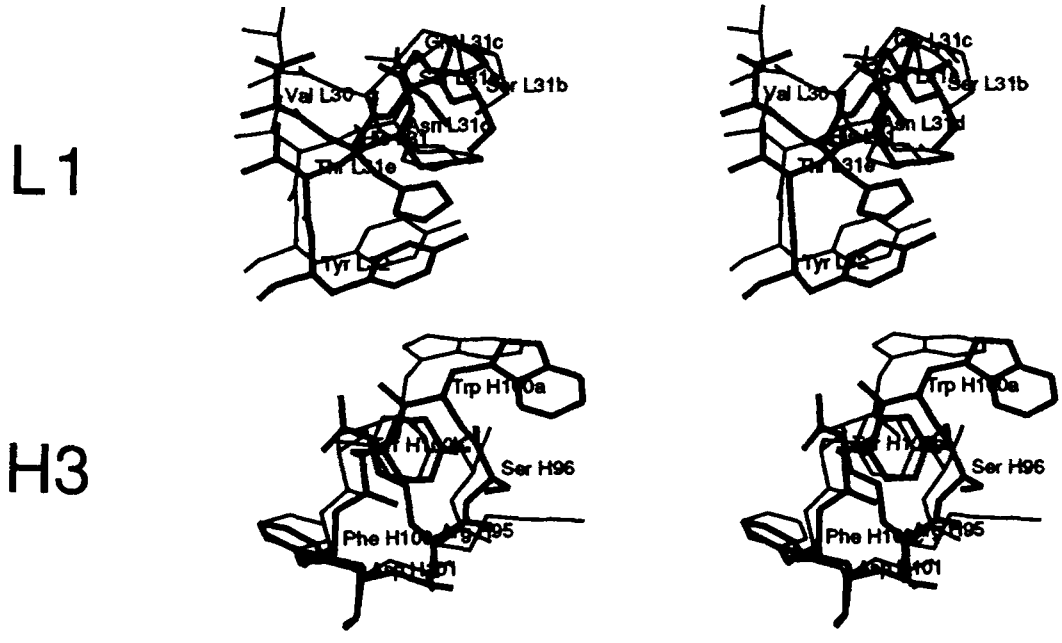

Fig. 6. Structure of the complementarity-determining loops L1 and H3 in the crystal structure of the TE33–CTP3 complex (thick lines) and in the calculated model used to derive the solution structure of bound CTP3 by NMR (thin lines). The two loops interact with each other in the calculated model but they do not in the crystal structure. The stacking interaction between Tyr L32 and Trp H100a is not observed in the crystal structure. These differences can be explained by the binding of a citrate ion in the vicinity of L1 in the crystal structure (see text).

formation (this distance is 3.7 and 4.5 Å in the crystal and calculated model, respectively). Consequently, the Tyr L32 ring is no longer available to interact with Trp H100a, which in turn swings out and becomes solvent exposed. As a result, Trp H100a in the crystal structure is no longer available to interact with the amide side chain of Gln 56 of bound CTP3. The bound peptide rearranges such that Gln 56 interacts with a series of polar residues on loops H1 and H2 as well as with a water molecule in the antigen-combining interface. This is the only water molecule, out of a total of 151 molecules, found to mediate the interaction between TE33 and CTP3 in the crystal structure of the complex (Shoham, 1993). In spite of the above-mentioned differences be-

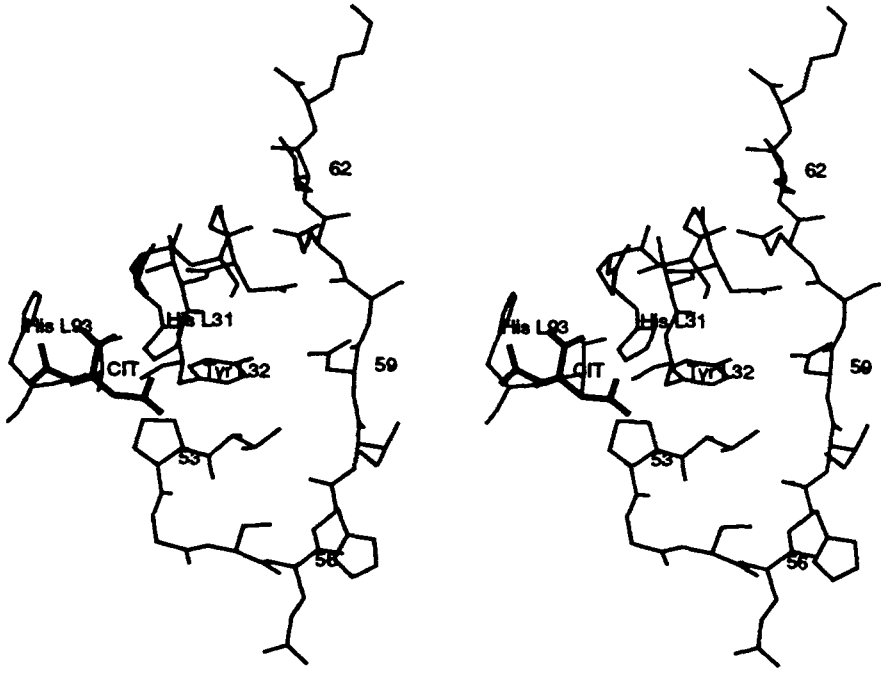

Fig. 7. A citrate ion (CIT) in the vicinity of the antigen-combining site in the crystal structure of the TE33–CTP3 complex. CTP3 residues are labeled by numbers only. The citrate forms van der Waals interactions with Pro 53 and polar interactions with residues from hypervariable loops L1 and L3. The central carboxylate group is hydrogen bonded to Ser L31a O^{γ}, and the two terminal carboxylate groups form salt bridges with the presumably positively charged imidazole rings of His L31 and His L98.

tween the crystal and NMR structures of bound CTP3, it should be noted that the structures are nonetheless similar (Fig. 5). The differences between solution and crystal structure in this case are less than reported, for example, for the high-resolution crystal and NMR structures of human recombinant interleukin-4 (Smith et al., 1994).

Comparison of the epitope conformation in the toxins and in the immunocomplexes

The conformation of the CTP3 epitope on LT and CT is different from that of CTP3-complexed-by-TE33 (Fig. 8; Kinemage 2). The β-turn, which in both the crystal and NMR structure of the TE33–CTP3 extends from Val 52 to Ser 55, is shifted by two residues in the toxins, from Gly 54 to His 57. Consequently, the conformation of His 57 is different in the toxins and in the antibody-peptide complexes. The imidazole ring of His 57 in CT and LT is located in between a β-strand and the central α-helix, forming polar interactions with Glu 51, Gln 56, the carbonyl oxygen of Gly 54, and a water molecule. In contrast, His 57 interacts directly with antibody moieties in the CTP3–TE33 complexes, where it is located in a hydrophobic pocket made up of Tyr H32 and Trp H100a (Shoham, 1993). Other differences exist in the conformation of Asp 59, which is solvent exposed in the toxins, whereas in the immunocomplexes it forms polar interactions with moieties on L1 and L2. This is not unexpected because residues involved in binding to the antibody should be solvent exposed in the free toxin. Conversely, the side chain of Lys 62 stabilizes the loop by forming a hydrogen bond with the backbone carbonyl oxygen of His 57 in LT, whereas it is solvent exposed in the crystal structure of TE33–CTP3 and disordered in the NMR structure.

The function of the CTP3 epitope is very different in the toxins and in the antipeptide complex. In CT and LT this loop carries functional groups that bind to the saccharide moiety on the receptor by an interaction of basically flat surfaces with protruding side chains. In the antipeptide complex, on the other hand, this loop has to fit snugly into a binding pocket. These are very different functional requirements that are a direct consequence of the different environments. The degree of conformational plasticity exhibited by this epitope is indeed remarkable.

Cross-reactivity of TE33 with intact CT

The antipeptide-antibody TE33 is cross-reactive with intact CT, but the binding constant for the intact toxin is a thousandfold lower (Anglister et al., 1988). Similar decrease in the affinity for the native proteins was observed for other antipeptide antibodies cross-reactive with the cognate protein (Berzofsky, 1985). What are the reasons for this decrease in the affinity of TE33 to CT? One possibility is that the amino- and/or carboxy-terminal charges of CTP3 are involved in antibody binding. These charges would, of course, not be present in the intact toxins. This is the case for TE34, another anti-CTP3 antibody that recognizes the carboxy-terminus of the peptide. TE34 does not bind CT at all, even in a solid-phase assay (Anglister et al., 1988). However, this possibility can be ruled out for TE33 because the termini are not involved in binding to the antibody. The first two residues are not seen in either the X-ray or the NMR structure. The very last and the last five residues are disordered in the crystal and NMR structures, respectively. Twelve residues from Val 52 to Lys 63 are seen in the crystal structure, and eight residues from Val 52 to Asp 59 are seen in the NMR structure.

Another potential reason for the affinity difference is that the conformation of the peptide-complexed-by-the-antibody is energetically less favorable compared to that of the peptide-in-the-toxin. That may well be the case because Te33-bound CTP3 exhibits unfavorable positive Φ values for Ser 55 and Gln 56 in the NMR and crystal structures, respectively (Scherf et al., 1992; Shoham, 1993). These residues are in left-handed α-helical conformations (Fig. 9A). Unfavorable dihedral angles do however, occasionally occur in proteins, especially near or at the active site (Herzberg & Moult, 1991). Gln 56 plays a pivotal role in the conformation of the bound peptide because it is a turning point in the chain and it makes numerous interactions with antibody moieties both in solution as well as in the crystalline state. On the other hand, Gln 56 is involved in galactose binding in

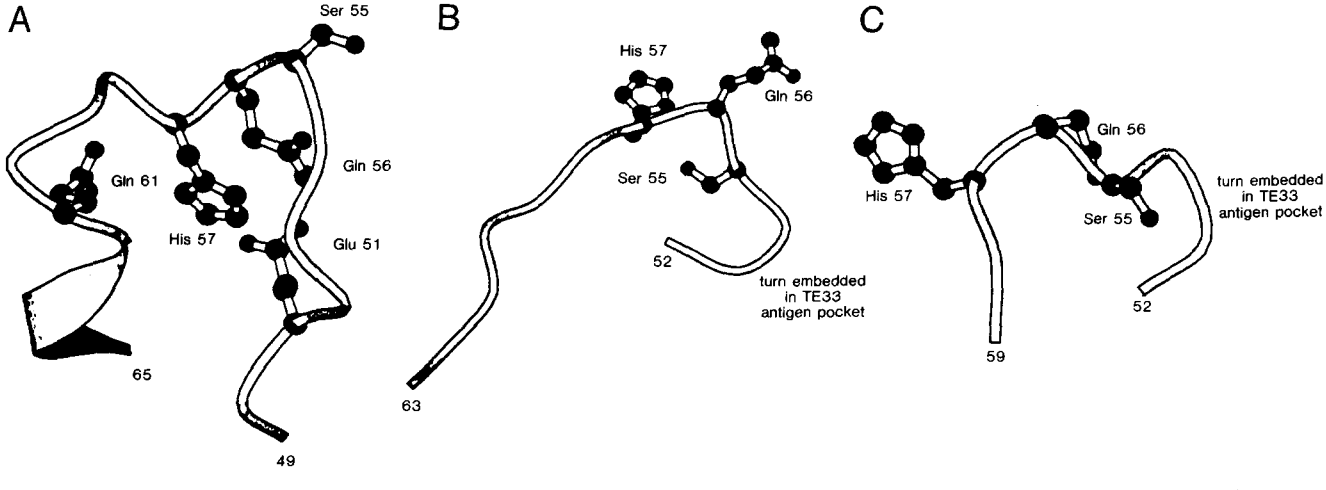

Fig. 8. Conformation of the CTP3 epitope in (**A**) the crystal structure of unliganded LT (Sixma et al., 1991), (**B**) the crystal structure of the antipeptide complex TE33–CTP3 (Shoham, 1993), and (**C**) the solution NMR-derived structure of the TE33–CTP3 complex (Scherf et al., 1992). For clarity, side chains are only shown for key residues.

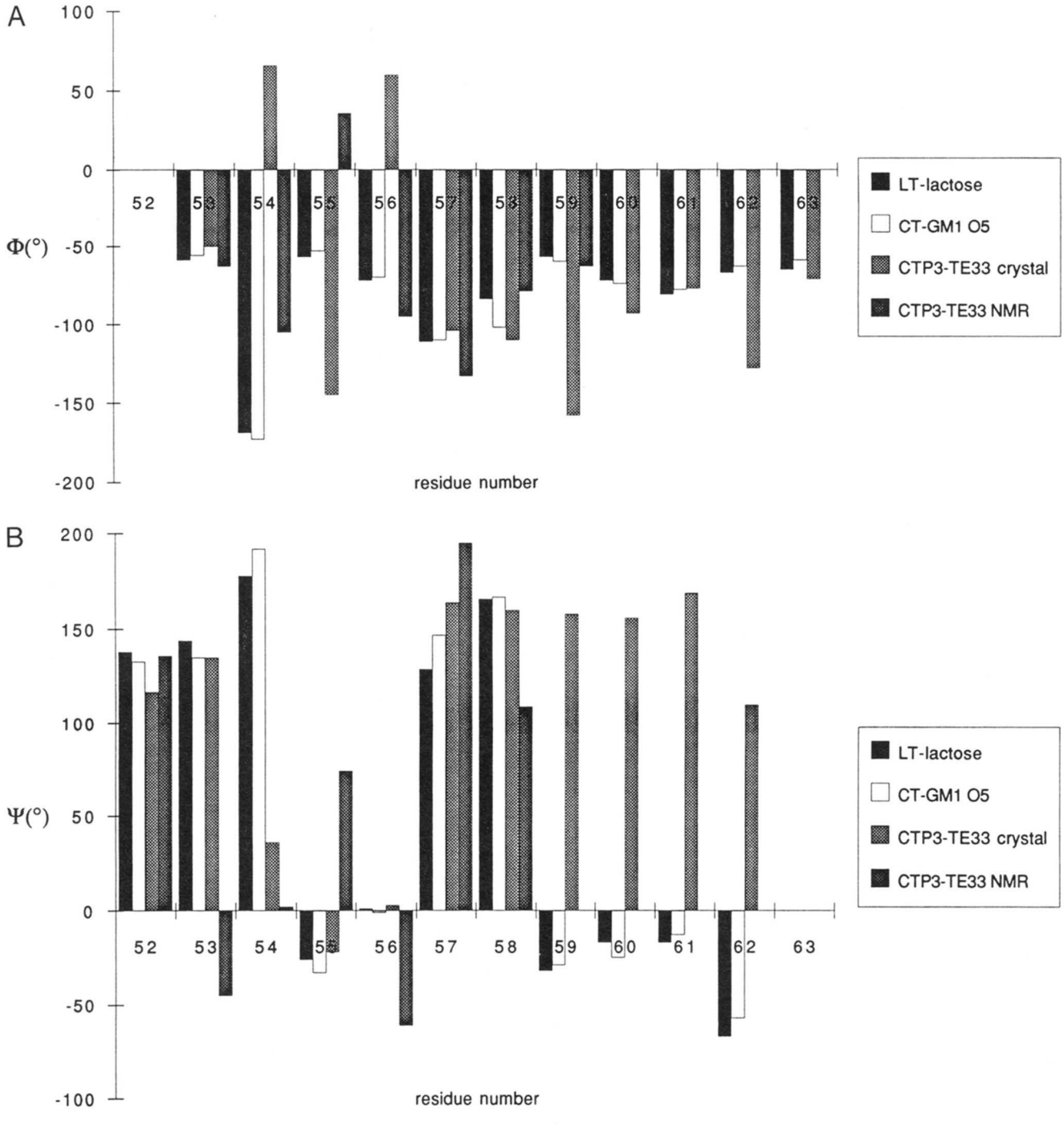

Fig. 9. Dihedral angles for CTP3 residues in four different structures: LT–lactose, lactose complex of LT from *E. coli*, first subunit of B pentamer (Sixma et al., 1992); CT–GM1 O5, G_{M1} pentasaccharide complex of CT B pentamer, first subunit (Merritt et al., 1994a); CTP3–TE33 crystal, crystal structure of CTP3 in complex with TE33 (Shoham, 1993); CTP3–TE33 NMR, NMR-derived solution structure of CTP3 in complex with TE33 (Scherf et al., 1992). **A:** ϕ angles. **B:** ψ angles.

both LT and CT and perhaps cannot adopt a conformation favorable for binding to TE33 without an energetically costly rearrangement.

Antibody binding of the peptide-in-solution implies partial dehydration of the peptide. Antibody binding of the peptide-in-the-toxin requires "detoxination" of the peptide-in-the-toxin. Several scenarios should be taken into account. We might hypothesize a process that involves unfolding of the toxin in order to allow the peptide-in-the-toxin to bind in the same conformation to the antibody as in the peptide–antibody complex, but then the remainder of the protein will be partially unfolded, which is certainly energetically unfavorable. This would be a major perturbation that would almost certainly lead to a much greater difference in affinity than the factor of a thousand ob-

served. So, a more likely scenario is that the antibody binds to the peptide-in-the-toxin in a different way than observed for the peptide-complexed-by-the-antibody. In the absence of an antibody–toxin structure, one can only assume that the interactions in the antibody–toxin complex would be quite different than in the peptide–antibody complex. A key question is how different? Are there parts of the peptide-in-the-toxin that adopt the same conformation as in the peptide-complexed-by-the-antibody? As shown in Figure 9 the only conserved conformation is for the dipeptide His 57-Ile 58. However, His 57 is buried in the toxins and hence it would be unavailable for binding to the antibody without a change in at least its side-chain dihedral angle(s). His 57 and the preceding Gln 56 are key residues in the interaction of CTP3 with TE33. It is possible that, upon interaction with the antibody, Gln 56 in the toxins rearranges to adopt a conformation as in the NMR-derived model for the peptide complex. Residues 60–64 may not interact with the antibody at all, or interact with the antibody in a manner different than observed in the crystal structure of the peptide–antibody complex. The possible reduced contact area and the required changes in the toxin conformation for antibody binding may account for the diminished affinity of TE33 to the toxin.

It is remarkable that despite the dramatic difference between the conformations observed for the CTP3 peptide bound to the TE33 Fab and for the equivalent peptide in the native toxin structure, the TE33 antibody nonetheless exhibits cross-reactivity with the native toxin. This observation is clearly relevant to the development of anticholera vaccines. The structural information available to us does not at present allow us to rule out a model for toxin–antibody association in which the CTP3 loop is substantially deformed from the conformation seen in the native toxin structures, nor does it rule out cross-reactivity based on binding of the native toxin conformation via a different set of specific binding interactions with the antibody than is seen in the CTP3–TE33 complex. In this respect it is interesting to note that, in the case of different steroids bound to the antiprogesterone antibody DB3, the cross-reactivity has been attributed to different binding orientations of the steroid rings without any major rearrangement either in the antibody or in the antigen (Arevalo et al., 1993). In another remarkable case of cross-reactivity of an antipeptide antibody to whole myohemerythrin, the peptide forms a β-turn conformation, whereas the identical sequence, embedded into the protein, forms an α-helix (Stanfield et al., 1990; Rini et al., 1992). Further insight into the issue of cross-reactivity might be gained by immunological and structural studies of toxin and peptide variants in which selected loop residues have been altered. This in turn could lead to a more efficient vaccine to intact CT B.

Acknowledgments

We thank Dr. Edwin Westbrook for providing us with CT coordinates prior to publication. This project was supported by grant S07 RR-05410-28 awarded by the Biomedical Research Support Grant Program, Division of Research Resources, NIH to M.S. Computations by M.S. on the CRAY Y-MP computer were supported by grant PDS153-2 from the Ohio Supercomputer Center. E.A.M. and W.G.J.H. thank the Murdoch Charitable Trust and the National Institutes of Health (grant AI 34501) for support.

References

Anglister J, Jacob C, Assulin O, Ast G, Pinker R, Arnon R. 1988. NMR study of the complexes between a synthetic peptide derived from the B subunit of cholera toxin and three monoclonal antibodies against it. *Biochemistry 27*:717–724.

Arevalo JH, Taussig MJ, Wilson IA. 1993. Molecular basis of crossreactivity and the limits of antibody–antigen complementarity. *Nature 365*: 859–863.

Berzofsky JA. 1985. Intrinsic and extrinsic factors in protein antigenic structure. *Science 229*:932–940.

Dallas WS, Falkow S. 1980. Amino acid sequence homology between cholera toxin and *E. coli* heat-labile toxin. *Nature 288*:499–501.

Herzberg O, Moult J. 1991. Analysis of the steric strain in the polypeptide backbone of protein molecules. *Proteins Struct Funct Genet 11*:223–229.

Jacob CO, Pines M, Arnon R. 1984a. Neutralization of heat-labile toxin of *E. coli* by antibodies to synthetic peptides derived from the B subunit of cholera toxin. *EMBO J 3*:2889–2893.

Jacob CO, Sela M, Arnon R. 1983. Antibodies against synthetic peptides of the B subunit of cholera toxin: Crossreaction and neutralization of the toxin. *Proc Natl Acad Sci USA 80*:7611–7615.

Jacob CO, Sela M, Pines M, Hurvitz S, Arnon R. 1984b. Both cholera-toxin induced adenylate cyclase activation and cholera toxin biological activity are inhibited by antibodies against related synthetic peptides. *Proc Natl Acad Sci USA 81*:7893–7896.

Levy R, Assulin O, Scherf T, Levitt M, Anglister J. 1989. Probing antibody diversity with 2D NMR: Comparison of amino acid sequences, predicted structures, and observed antibody–antigen interactions in complexes of two antipeptide antibodies. *Biochemistry 28*:7168–7175.

Merritt EA, Murphy MEP. 1994. Raster3D version 2.0—A program for photorealistic molecular graphics. *Acta Crystallogr D 50*:869–873.

Merritt EA, Sarfaty S, van den Akker F, L'Hoir CE, Martial JA, Hol WGJ. 1994a. Crystal structure of cholera toxin B-pentamer bound to receptor G_{M1} pentasaccharide. *Protein Sci 3*:166–175.

Merritt EA, Sixma TK, Kalk KH, van Zanten BAM, Hol WGJ. 1994b. Galactose-binding site in *E. coli* heat-labile enterotoxin (LT) and cholera toxin (CT). *Mol Microbiol 13*:745–753.

Rini JM, Schulze-Gahmen U, Wilson IA. 1992. Structural evidence for induced fit as a mechanism for antibody–antigen recognition. *Science 255*:959–965.

Satow Y, Cohen GH, Padlan EA, Davies DR. 1987. Phosphocholine binding immunoglobulin Fab MCP603. An X-ray diffraction study at 2.7 Å. *J Mol Biol 190*:593–604.

Scherf T, Hiller R, Naider F, Levitt M, Anglister J. 1992. Induced peptide conformations in different antibody complexes: Molecular modeling of the three-dimensional structure of peptide–antibody complexes using NMR-derived distance restraints. *Biochemistry 31*:6884–6897.

Shoham M. 1993. Crystal structure of an anticholera toxin peptide complex at 2.3 Å. *J Mol Biol 232*:1169–1175.

Sixma TM, Pronk SE, Kalk KH, van Zanten BAM, Berghuis AM, Hol WGJ. 1992. Lactose binding to heat-labile enterotoxin revealed by X-ray crystallography. *Nature 355*:561–564.

Sixma TK, Pronk SE, Kalk KH, Wartna ES, van Zanten BAM, Witholt B, Hol WGJ. 1991. Crystal structure of a cholera toxin-related heat-labile enterotoxin from *E. coli*. *Nature 351*:371–377.

Smith LJ, Redfield C, Smith RAG, Dobson CM, Clore GM, Gronenborn AM, Walter MR, Naganbushan TL, Wlodawer A. 1994. Comparison of four independently determined structures of human recombinant interleukin-4. *Nature Struct Biol 1*:301–310.

Stanfield RL, Fieser TM, Lerner RA, Wilson IA. 1990. Crystal structures of an antibody to a peptide and its complex with peptide antigen at 2.8 Å. *Science 248*:712–719.

Yamamoto T, Gojobori T, Yokota T. 1987. Evolutionary origin of pathogenic determinants in enterotoxigenic *E. coli* and *Vibrio cholerare* O1. *J Bacteriol 169*:1352–1357.